WINDOWS INTO SAUROPSID AND SYNAPSID EVOLUTION
Essays in honor of Prof. Louis L. Jacobs, pp. 222–232, 2023

INSIGHT ON INTERACTIONS AMONG CLIMATIC, BIOTIC, AND ATMOSPHERIC PROCESSES DURING THE MID-CRETACEOUS USING TERRESTRIAL DEPOSITS IN TEXAS AND OKLAHOMA

KATE A. ANDRZEJEWSKI[1,]*, ANDREAS MÖLLER[2], and CHRISTOPHER R. NOTO[3]

[1]Kansas Geological Survey, University of Kansas, Lawrence, Kansas, 66047, U.S.A., geokate@ku.edu;
[2]Department of Geology, University of Kansas, Lawrence, Kansas, 66045, U.S.A., amoller@ku.edu;
[3]Deparment of Biological Sciences, University of Wisconsin-Parkside, Kenosha, Wisconsin, 53141, U.S.A., noto@uwp.edu

ABSTRACT Chemical, mineralogical, and stable isotopic proxies are applied to reconstruct paleoclimatic and paleoatmospheric conditions during the Mid-Cretaceous (Aptian-Cenomanian) using terrestrial deposits from fossil localities in north-central Texas and southern Oklahoma. These results in conjunction with analyses of the $\delta^{13}C$ of plant organic material at each locality are compared to investigate interactions between biotic responses in plant organic matter to changes in paleoprecipitation and paleoatmospheric pCO_2. Results show a strong correlation between mean annual precipitation (MAP) and the $\delta^{13}C$ of plant organic matter. Localities reporting low paleoprecipitation estimates correlate with more positive $\delta^{13}C$ organic matter values, consistent with modern observations. Less understood and constrained is the influence of changes in pCO_2 levels on $\delta^{13}C$ of plant organic matter. Using paleosol carbonates, we show a decrease in $\delta^{13}C$ of occluded organic matter associated with increases in estimated atmospheric pCO_2 levels, with an estimated pCO_2 effect of -0.9‰ ± -0.5‰ per 100 ppmV on the $\delta^{13}C$ values of organic matter collected from two localities with similar paleoprecipitation estimates. U-Pb dating of zircon collected from the Jones Ranch locality indicates a maximum depositional age of 113.1 ± 1.5 Ma (n=4). This provides the first reported absolute age for the Twin Mountains Formation and is a valuable time constraint for a reported increase in atmospheric pCO_2 occurring at the Aptian/Albian boundary and at the onset of the OAE1b interval. Together these data exhibit how deep time proxies from terrestrial deposits can contribute to our knowledge and understanding of interactions among biotic, climatic, and atmospheric processes while also providing crucial paleoclimatic and paleoatmospheric data for periods of greenhouse climate conditions.

KEYWORDS Cretaceous, Paleoclimate, Paleosols, Stable Isotopes, Maximum depositional age

INTRODUCTION

The transition from Lower to Upper Cretaceous deposits in Texas and Oklahoma captures significant changes in the biologic, climatic, and geographic spheres at both regional and global scales. Regionally, this includes dynamic evolutionary changes with major faunal turnover events among archosaurs and mammals, the rise of angiosperms, and the first appearance of snakes and marsupial taxa (Jacobs and Winkler, 1998; Winkler et al., 2015). Additionally, these biotic changes occur during intervals of major paleogeographic changes with a transgression of the Glen Rose Sea onto the Texas craton around the Aptian/Albian boundary, followed by the formation and completion of the Western Interior Seaway (Haq et al., 1987; Kauffman and Caldwell, 1993; Slattery et al., 2015). Globally, this time frame (Aptian-Cenomanian) also encompasses several major perturbations in the global carbon cycle, which are associated with the widespread development of anoxic-euxinic conditions in the ocean basins, known as Ocean Anoxic Events (OAE's; Schlanger and Jenkyns 1976; Jenkyns, 1980, 2010; Arthur et al. 1987; Schlanger et al.; 1987). These include the Early Albian OAE1b (Jenkyns, 2010), the Albian-Cenomanian OAE1d (Gröcke et al., 2006; Richey et al., 2018), and the mid-Cenomanian Event (MCE; Coccioni and Galeotii, 2001). Several studies have attempted to place these events in the context of abiotic and biotic factors including regional paleogeographic changes with the formation and completion of the Western Interior Seaway (Jacobs and Winkler 1998, Winkler et al., 2015) and changes in paleoclimate (Andrzejewski & Tabor, 2020).

*Corresponding author

Deciphering the influence of regional and global changes in deep time is difficult given numerous factors including incomplete sedimentary records, uncertainty in stratigraphic correlation, and varied sample preservation. Paleosols constitute a large part of the terrestrial sedimentary record and thus provide a wealth of information regarding Earth history (Retallack, 1986). Paleosols capture slices of geologic time and provide a unique interface where biotic, climatic, and atmospheric processes interact. This allows paleosols to record important factors that can be used to reconstruct paleoenvironment and estimate paleotemperature, paleoprecipitation, terrestrial organic matter carbon values, paleoatmospheric pCO_2 levels, and absolute geologic age (e.g. Sheldon and Tabor, 2009; Tabor and Myers, 2015, Tabor et al., 2017; Smith et al., 2017; Joeckel et al., 2023). Given the preservation of paleosols in terrestrial units during the transition from Lower to Upper Cretaceous in Texas and Oklahoma, we apply current methodologies and developed proxies to investigate the possible influences of regional and global paleoprecipitation and paleoatmospheric pCO_2 on changes in the $\delta^{13}C$ of terrestrial organic matter.

GEOLOGICAL SETTING

This study analyzes data collected from 5 localities, spanning the Lower to Upper Cretaceous (Aptian-Cenomanian) stratigraphy of north-central Texas and southern Oklahoma. This includes two fossil localities from the Twin Mountains Formation in north-central Texas: Proctor Lake (PL) and Jones Ranch (JR), one locality in the Antlers Formation of southern Oklahoma: (CR), and two localities in the Woodbine Group in north-central Texas: the Arlington Archosaur Site (AAS), and Acme Brick Pit (ABP) (Fig. 1). Correlation of these localities is difficult as the succession includes the time-transgressive progradational-retrogradational sequence of the Western Interior Seaway. However, the stratigraphic analysis by Jacobs and Winker, (1998) provides sufficient constraints to place these localities within a framework that ensures chronological order, albeit without chronometric dates (Fig. 1). Andrzejewski and Tabor, (2020) and Andrzejewski et al., (2022) report data from paleosols sampled at these localities including paleoprecipitation, paleotemperature, and atmospheric pCO_2 estimates which will be referenced herein.

The Twin Mountains Formation represents the lowest Cretaceous deposits in north-central Texas and lies unconformably upon Pennsylvanian and Permian strata (Young, 1967). The overlying Glen Rose Formation contains ammonite faunas used to define the Aptian-Albian boundary indicating the Twin Mountains Formation is Aptian in age (Young, 1967; Scott, 1940; Young, 1974; Young 1986). Exposures of the Twin Mountains Formation have been interpreted as sedimentary deposits of meander belt fluvial systems transitioning stratigraphically upward to marginal marine deposits (Hall, 1976). The Proctor Lake locality lies approximately 17 m above the Pennsylvanian contact and 35 m below the Glen Rose Formation contact. The Jones Ranch fossil locality occurs stratigraphically higher in the Twin Mountains Formation, occurring approximately 9.7 m below the Glen Rose Formation contact. Morphology and data produced from the paleosols sampled from these localities are described in Andrzejewski and Tabor (2020) and Andrzejewski et al. (2022).

The marine-dominated Glen Rose Formation pinches out to the north, juxtaposing the terrestrial-dominated Twin Mountains and Paluxy Formations which combine to form the Antlers Formation (Fig. 1). The Antlers Formation contains claystone layers with unconsolidated sandstone lenses and carbonate concretions that have been interpreted as fluvial, deltaic, and strandplain settings (Winkler et al.1990; Hobday et al. 1981). The absence of the Glen Rose Formation as a biostratigraphic marker makes it difficult to determine precise stratigraphic positions of localities within the Antlers Formation. Locality CR sampled in southern Oklahoma is stratigraphically equivalent with the fossil locality OMNH V706, which is considered to be located in the middle of the Antlers Formation, approximately 87 m above the base and stratigraphically above the PL and JR localities (Cifelli et al., 1997).

The Woodbine Group has a long history of revisions in stratigraphic subdivision and nomenclature based on differing interpretations of surface exposures versus subsurface drill cores and wireline logs (Ambrose et al. 2009; Berquist, 1949; Dodge 1952; Dodge 1968; Hentz et al. 2014; Johnson, 1974; Murlin, 1975; Oliver, 1971; Trudel, 1994). Current stratigraphic subdivision recognizes two units: the Dexter and Lewisville Formations. The lower Dexter Formation represents marginal and marine environments (Berquist, 1949; Dodge, 1952; Dodge 1968; Dodge, 1969; Johnson, 1974; Oliver, 1971) while the overlying Lewisville Formation represents a low-lying coastal plain (Main, 2009; Oliver, 1971; Powell, 1968). Both the Arlington Archosaur Site and Acme Brick Pit localities occur in the middle to upper Lewisville Formation.

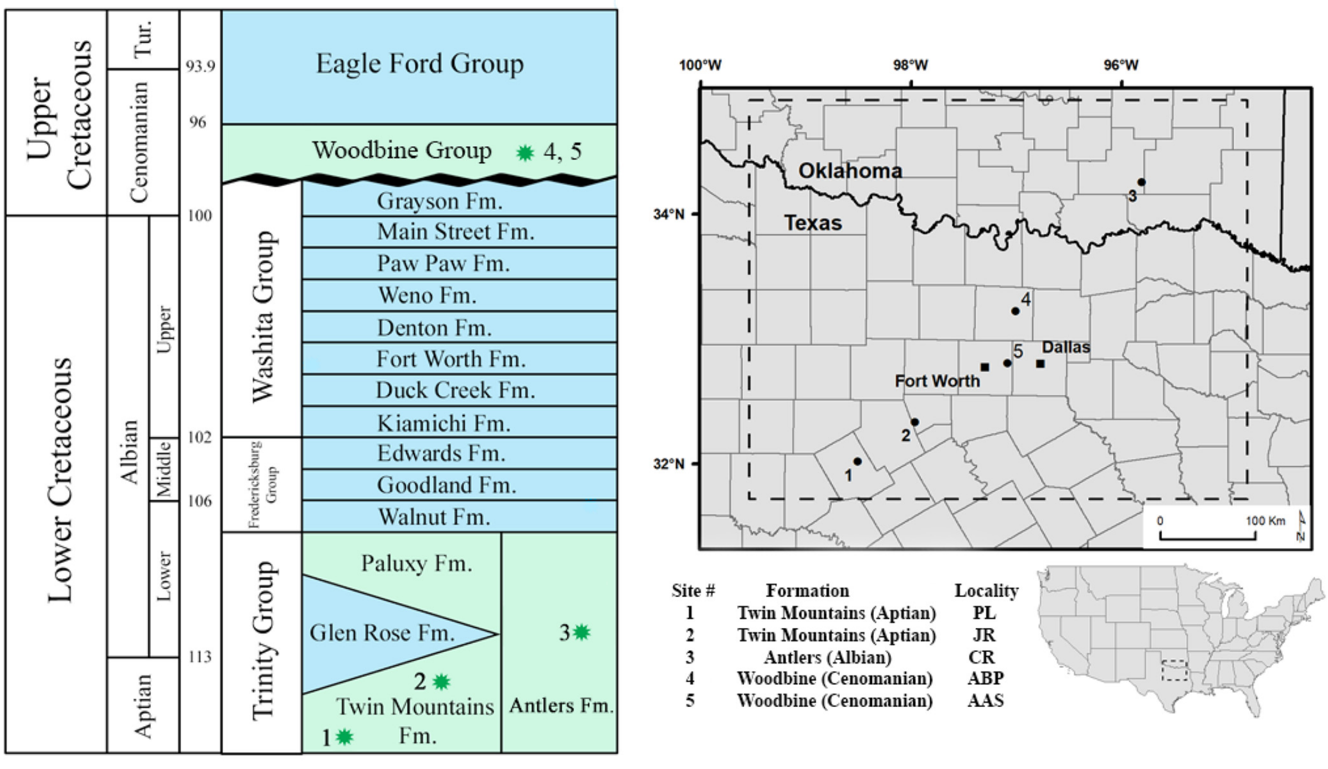

(A) (B)

FIGURE 1. Regional stratigraphic column and map of study area: (A) lithostratigraphic units spanning the Early to Late Cretaceous interval of north-central Texas and southern Oklahoma (modified from Jacobs and Winkler, 1998). (B) map displaying the study area with localities correlating to the site number listed with collected samples: 1 = Proctor Lake locality (PL), 2 = Jones Ranch locality (JR), 3 = Cross locality (CR), 4 = Acme Brick Pit (ABP), 5 = Arlington Archosaur Site (AAS).

Due to lack of surface exposures and chronostratigraphic constraint exact stratigraphic relationship between the two localities cannot be determined. The presence of the ammonite *Conlinoceras tarrantense* has been used to indicate an early middle Cenomanian age (~96 Ma) for Lewisville Formation strata (Kennedy and Cobban, 1990; Emerson et al., 1994; Lee, 1997a, b; Jacobs and Winkler; 1998; Gradstein et al., 2004). However, Ambrose et al., (2009) suggest that upper portions of the Lewisville Formation were deposited during the late Cenomanian, with overall deposition of the Woodbine Group ending around 92 Ma. Andrzejewski and Tabor, (2020) contains descriptions of the Arlington Archosaur Site and Acme Brick Pit, including detailed descriptions of the sampled paleosols.

METHODS

Bulk paleosol samples were collected approximately every 10 cm from the measured section at the Arlington Archosaur Site. Two bulk samples were collected at the Acme Brick Pit site, one from the paleosol B horizon and one 15 cm above the B horizon. New $\delta^{13}C$ values for bulk sedimentary organic matter reported from the Woodbine Group were produced at the Keck Palaeoenvironmental and Environmental Stable Isotope Lab at the University of Kansas. Samples were powdered with mortar and pestle to generate approximately 1 g of powder. Samples were then decarbonated with 0.5 M hydrochloric acid for at least 24 h or until samples no longer reacted with fresh acid. Samples were then rinsed with deionized water by centrifugation and decanting until no longer acidic. Rinsed samples were then dried at 50°C. Approximately 0.3-2 mg per sample were combusted with a Costech elemental analyzer, with the resulting CO_2 analyzed with a ThermoFinnigan MAT 253 continuous-flow isotope ratio mass spectrometer. All samples are reported relative to V-PDB, with accuracy monitored by analysis of internal standards IAEA-600 and USGS 24 to within 0.1‰. Methodology for previously reported chemical, mineralogical, and stable isotopic analyses can be found in Andrzejewski and Tabor, (2020) and Andrzejewski et al. (2022).

A 5 cm interval of bulk paleosol sample collected approximately 50 cm below the top of the B horizon from the Jones Ranch Quarry was selected for detrital zircon U-Pb geochronology. Zircon grains were separated from bulk paleosol material at the University of Kansas Isotope Geochemistry Laboratories by a combination of chemical and physical disaggregation and heavy-mineral separation techniques including a disk mill, ultrasonic bath (Hoke et al. 2014), Frantz™ isodynamic magnetic separator, and heavy liquids (methylene iodide). At least 175 grains were handpicked under a binocular microscope and mounted on double sided tape. The purpose of the investigation is determination of the age of deposition based on the premise that mature paleosols may be cryptotephra, as they can capture volcanic zircons during the time period of soil formation (Smith et al., 2017 Joeckel et al., 2023). During grain picking preference was therefore given to euhedral, unabraded, colorless, zircons to maximize the chance to find the youngest, non-detrital zircons. Results for older, detrital grains are therefore not providing an unbiased sample of the entire detrital population, but only a qualitative example of older populations, and should not be used in statistical comparisons and likeness tests. U-Pb zircon ages were determined by laser ablation inductively coupled plasma mass spectrometry (LA-ICP-MS) using a Photon Machines Analyte G2 193 nm ArF excimer laser ablation system coupled with a Thermo Scientific Element2 ICP-MS. Circular 15 μm spots were ablated with the laser at 1.3 J/cm^2 fluence with a 10 Hz repetition rate for 25 seconds, and ablated material was carried to the ICP-MS in helium gas with a 1 L/min combined flow rate. Downhole elemental and isotopic fractionation and calibration drift were corrected by bracketing measurements of unknowns with zircon reference materials using the IOLITE software package (Paton et al., 2011) and the VizualAge data reduction scheme (Petrus and Kamber, 2012). Zircon GJI (Jackson et al., 2004) was used for calibration, the zircon reference materials Plesovice (Sláma et al., 2008), Fish Canyon Tuff (FCT, Wotzlaw, 2013), Duluth Gabbro (FCSZ, Paces and Miller, 1993) were used to validate the calibration. All reference materials matched the published ages within 1% uncertainty. Analytical results are presented using Isoplot (Vermeesch, 2018). The maximum age of deposition was determined from the youngest population of grains. Kernel density estimates (KDEs) were produced using DensityPlotter 7.1 (Vermeesch 2012).

RESULTS

The $\delta^{13}C$ of bulk sedimentary organic matter collected from two localities in the Woodbine Group ranged from −22.2 to −26.1‰ with an average of −24.6‰ reported from 23 samples (Table 1). The $\delta^{13}C$ values reported for organic matter in the Woodbine Group are consistent with C3 vegetation shown to dominate the Cretaceous landscape (Koch, 1998). These reported values are combined with previous analyses of organics occluded in paleosol carbonate nodules from Andrzejewski et al. (2022) and shown in Fig. 2(A). While comparing the $\delta^{13}C$ of plant organic matter, we note that results from Myers et al. (2016) indicate an ~1‰ offset between average $\delta^{13}C$ values of bulk and occluded organic matter; however, this offset is far less than the overall range $\delta^{13}C$ values of plant organic matter reported at the localities and does not affect the results of the produced chemostratigraphic profile. Results from this combined chemostratigraphic profile show a sharp decrease of ~3.0‰ in the mean $\delta^{13}C$ of organic matter from the Proctor Lake locality to the Jones Ranch locality in the Twin Mountains Formation. This is followed by a smaller decrease in the mean $\delta^{13}C$ of organic matter of ~0.6‰ from the Jones Ranch locality in the Twin Mountains formation to the Oklahoma localities in the Antlers Formation. The mean $\delta^{13}C$ of organic matter between localities in the Antlers Formation and the Woodbine Group appear to be fairly consistent with their mean values overlapping.

Results showing the concordia ages of the 4 youngest concordant zircon grains from a total population of 175 zircon grains analyzed from the Jones Ranch locality in the Twin Mountains Formation are shown in Figs. 3 and 4. The youngest four overlapping zircon U-Pb results from this population (2.3% of total) yield a maximum depositional age of 113.1 ± 1.5 Ma. Microscope images of these four euhedral zircon grains are shown in Fig. 3, indicating minimal detrital transport of these grains. This age fits within the span of the Aptian/Albian stage boundary and is consistent with previously reported age estimates of the locality based on stratigraphic relationship and overlying biostratigraphic markers in the Glen Rose Formation (Young, 1967; Scott, 1940; Young,

TABLE 1. Measured $\delta^{13}C$ of organic matter ($\delta^{13}C_{OM}$ ‰ VPDB), of acid-treated bulk paleosol samples from the Woodbine Group (Cenomanian)

Location	Sample	Formation (Age)	$\delta^{13}C_{om}$ (‰ VPDB)
Arlington Archosaur Site	15CS717-1	Woodbine Group (Cenomanian)	-24.15
	15CS717-2		-26.09
	15CS717-3		-23.58
	15CS717-4		-25.19
	15CS717-5		-22.22
	15CS717-6		-24.98
	15CS717-7		-24.21
	15CS717-8		-25.42
	15CS717-9		-23.62
	15CS717-10		-24.58
	15CS717-11		-24.08
	15CS717-15		-23.28
	15CS717-17		-24.24
	15CS717-18		-25.01
	15CS717-19		-24.69
	15CS717-20		-25.03
	15CS717-21		-25.73
	15CS717-9 proximal end		-23.44
	15CS717-9 middle		-24.00
	15CS717-9 distal end		-23.69
	AA1		-25.59
Acme Brick Pit		Woodbine Group (Cenomanian)	
	Above ABP		-25.92
	ABP B Horizon		-25.83

1974; Young, 1986). These results provide the first absolute age determined for the upper Twin Mountains Formation and the Jones Ranch fossil locality.

DISCUSSION

The $\delta^{13}C$ or plant organic matter is thought to be influenced by several factors, the most influential being mean annual precipitation (Swap et al., 2004; Schulze et al., 1998). Modern studies show C_3 plants that are water stressed and receive lower amounts of mean annual precipitation correlate with more positive $\delta^{13}C$ values (Kohn, 2010; Ma et al., 2012). The Cretaceous record in Texas and Oklahoma is consistent with this relationship, as shown by the $\delta^{13}C$ of organic matter results of this study and Andrzejewski et al. (2022) in relation to paleoprecipitation estimates produced by Andrzejewski and Tabor (2020) (Fig. 2). The PL locality recorded the most positive $\delta^{13}C$ organic matter values, averaging −21.3‰ which correlate to the lowest MAP estimates averaging 331 ± 110 mm/yr. Localities in the Antlers Formation and Woodbine Group with significantly higher MAP estimates ranging from 952 ± 110 to 1486 ± 110 mm/yr contain more negative $\delta^{13}C$ organic matter values ranging from −23.3 to −26.1‰. These periods of higher estimated mean annual precipitation correspond to and are likely driven by various transgressions onto the Texas craton during sea level

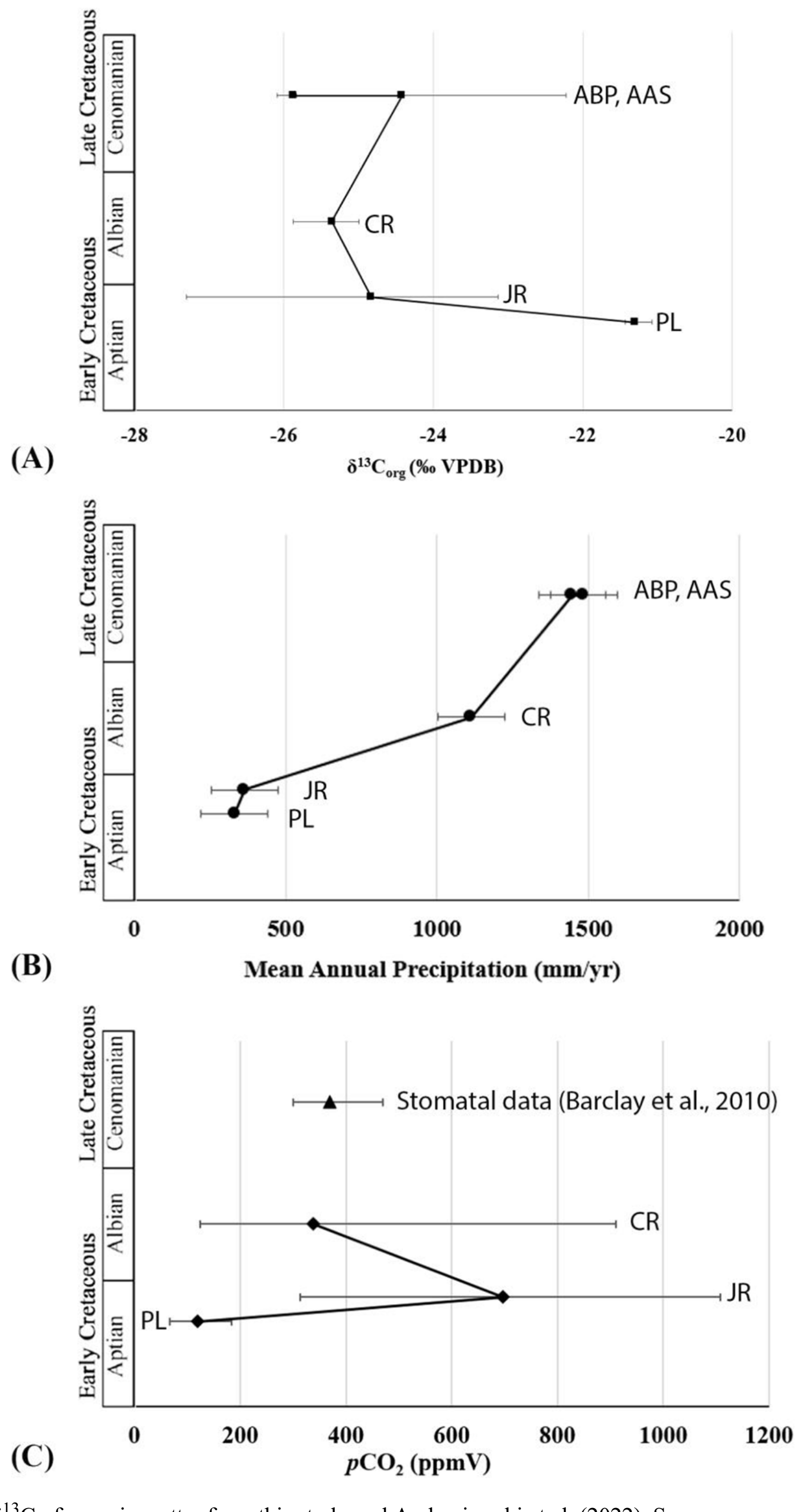

FIGURE 2. (A) Measured $\delta^{13}C$ of organic matter from this study and Andrzejewski et al. (2022). Squares represent the mean $\delta^{13}C$ of organic matter of each locality and error bars show minimum and maximum values recorded. (B) Mean annual precipitation estimates for each locality produced from weathering proxies of bulk paleosol material (Andrzejewski and Tabor 2020). Circles represent estimated value with a reported error of ±110 mm/yr. (C) Atmospheric pCO_2 estimates produced from paleosol carbonates at localities PL, JR, and CR with mean estimates represented as diamonds and error bars showing minimum and maximum estimated values (Andrzejewski et al. 2022). Atmospheric pCO_2 estimates produced from stomatal data from Cenomanian deposits in Utah with mean estimate represented as triangle with error bars showing minimum and maximum estimated values (Barclay et al., 2010).

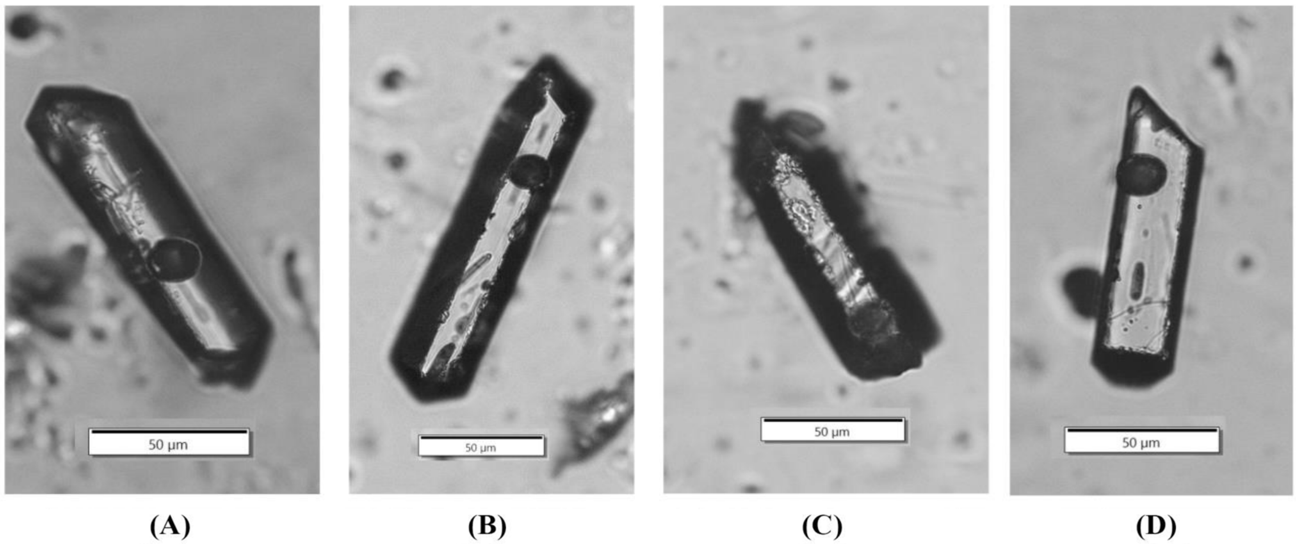

FIGURE 3. Microscopic images of the youngest population of zircon grains analyzed from the Jones Ranch locality in the Twin Mountains Formation. Note circles on the grains where laser ablation sample was targeted. Scale bar equals 50 µm.

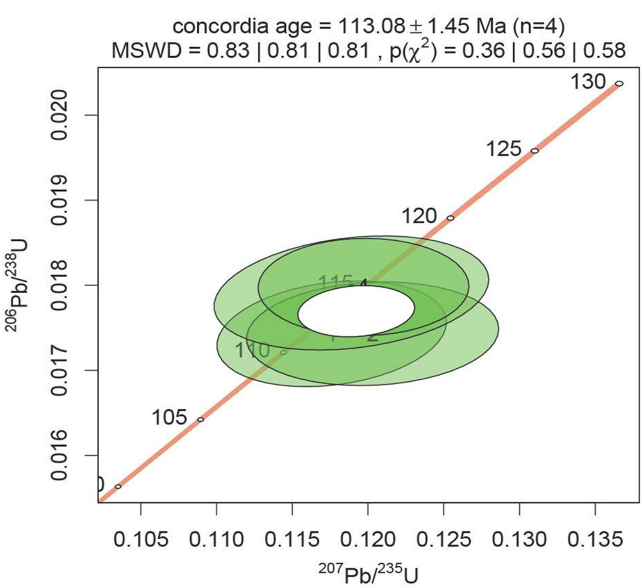

FIGURE 4. Concordia plot of youngest population of zircon grains (n = 4) collected from the Jones Ranch locality in the Twin Mountains Formation. Analysis reveals an age of 113.1 ± 1.45 MA.

highstands, which provided new moisture sources (Andrzejewski and Tabor, 2020). However, mean annual precipitation does not explain the significant decrease in the $\delta^{13}C$ of organic matter between the PL and JR localities in the Twin Mountains Formation as both exhibit similar MAP estimates of 331 ± 110 and 365 ± 100 mm/yr respectively.

The lack of consistency between precipitation and the $\delta^{13}C$ of plant organic matter when comparing the PL and JR localities leads to the less understood and constrained influence that changes in atmospheric pCO_2 levels have on the $\delta^{13}C$ of plant organic matter. While the relationship between fluctuating atmospheric pCO_2 levels and the $\delta^{13}C$ of plant organic matter is still debated, two recent studies have shown a negative correlation, with increased atmospheric pCO_2 levels corresponding to more negative $\delta^{13}C$ signatures in plant organic matter (Breecker, 2017; Hare et al. 2018). A study by Hare et al. (2018) found a pCO_2 effect on the $\delta^{13}C$ of organic matter in gymnosperms of −1.4 ± 1.2‰ per 100ppmV during the last deglaciation using ice cores and fossil plant materials. Results from Breecker (2017) found a pCO_2 effect on the $\delta^{13}C$ of organic matter of −1.6 ± 0.3‰ per 100 ppmV (1σ) during the Quaternary using data collected from speleothems. Atmospheric pCO_2 estimates produced in Andrzejewski et al. (2022) using paleosol carbonates show a significant increase between the PL and JR localities in the Twin Mountains Formation with atmospheric pCO_2 from locality PL ranging from 67-183 ppmV to locality JR ranging from 313-1108 ppmV (Fig. 2). Given that both the PL and JR localities have similar paleoprecipitation estimates yet show a negative shift of ~3.5‰ in the $\delta^{13}C$ of organic matter it provides an opportunity to estimate the influence of changes in atmospheric pCO_2 levels on the $\delta^{13}C$ of organic matter during the Early Cretaceous. When the average pCO_2 estimates from the PL and JR localities are combined with the negative 3.5‰ shift

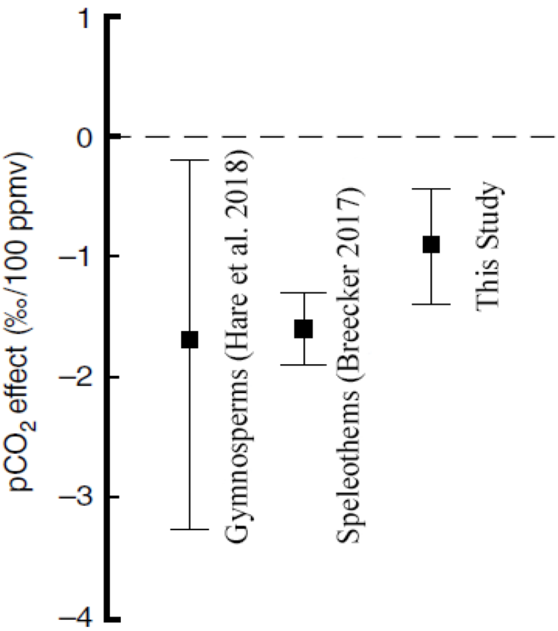

FIGURE 5. Effect of atmospheric pCO_2 on mean stable carbon isotope composition of plant organic matter (modified from Hare et al., 2018). Estimate from Hare et al. (2018) include data produced from gymnosperms from the last deglaciation. Estimate from Breecker (2017) include data from speleothems from the Quaternary. Estimate from this study include data from paleosol carbonates during the Aptian/Albian.

in organic carbon values it reveals a pCO_2 effect on the $\delta^{13}C$ of organic matter of −0.9 ± 0.5‰ per 100ppmV (Fig. 5). This range appears consistent with the studies conducted by Hare et al. (2018) and Breecker (2017). Notably, these results confirm the direct influence of global atmospheric processes on terrestrial organic carbon in deep time.

To further investigate the significant increase in atmospheric pCO_2 a bulk paleosol sample was collected from the JR locality to extract and date zircon grains by the U-Pb method. Paleosols have been shown to be a great source for volcanic zircon, yielding U-Pb ages close to the age of deposition (e.g. Smith et al. 2017). Many paleosols can be referred to as cryptotephras. While they may not stand out as immediately recognizable volcanic ash deposition in the field like white bentonite clay layers, they may contain microscopic fragments from volcanic tephra deposits that can be separated and analyzed using technical laboratory techniques (Davies, 2015; Joeckel et al., 2023). Results from the analyzed 175 zircon grains in this study revealed a youngest population consisting of 4 grains to produce a maximum depositional age of 113.1 ± 1.5 Ma. This age provides the first absolute age for this important fossil locality and confirms its geochronological position near the Aptian/Albian boundary. Furthermore, it confirms a rapid rise in atmospheric pCO_2 near the onset of ocean anoxic event 1b (OAE1b: 113-109 Ma; Leckie et al. 2002). Several black-shales have been identified and described as events within OAE1b including the 113/Jacob (Aptian), the Kilian (Aptian-Albian boundary), the Paquier (Albian), and the Lenhardt (Albian) (Leandro et al. 2022). While the current sample set of one zircon U-Pb maximum depositional age does not provide the resolution needed to correlate the changes in atmospheric pCO_2 with any of these specific events, future work including extraction of zircon from multiple samples from the remaining fossil localities and increasing precision of the dates using the CA-ID-TIMS dating techniques would provide the clarity needed to understand climatic and atmospheric shifts and their association with global carbon events. Increased age resolution could also be provided by improving stratigraphic coverage through obtaining and analyzing core samples in the study area. Together, the presented dataset confirms how deep time proxies from paleosols can contribute to our understanding of climatic, atmospheric, and biological processes during earth's history including critical periods where greenhouse climatic conditions persisted and highlight the necessity for continued study.

CONCLUSION

Data produced from chemical, mineralogical, and stable isotopic analyses from Mid-Cretaceous (Aptian-Cenomanian) paleosols sampled from fossil localities in north-central Texas and southern Oklahoma reveal insight into the biotic response of the $\delta^{13}C$ of plant organic matter to changes in estimated mean annual precipitation and atmospheric pCO_2. Localities reporting low paleoprecipitation estimates correlate with more positive $\delta^{13}C$ organic matter values while localities reporting high paleoprecipitation estimates correlate with more negative $\delta^{13}C$ organic matter values which is consistent with observations in modern systems. The changes in estimated mean annual precipitation appear to be related to regional transgressive/regressive events, with higher mean annual precipitation estimates occurring due to new moisture sources provided by various transgressions onto the Texas craton during sea level highstands. To understand and constrain the influence of changes in atmospheric pCO_2 levels on the

$\delta^{13}C$ of plant organic matter, paleosol carbonates from two localities (Proctor Lake and Jones Ranch) with consistent mean annual precipitation estimates but significant differences in estimated atmospheric pCO_2 estimates were used to estimate a pCO_2 effect of −0.4 to −1.4‰ per 100 ppmV on the $\delta^{13}C$ values of organic matter. U-Pb dating of zircon collected from the Jones Ranch locality indicates a maximum depositional age of 113.1 ± 1.5 Ma (n = 4, Figs. 3, 4). This provides the first reported absolute age dating for the Twin Mountains Formation and is a valuable time constraint for a reported increase in atmospheric pCO_2 occurring at the Aptian/Albian boundary and near the onset of the OAE1b interval suggesting a global influence on the $\delta^{13}C$ of terrestrial plant organic matter. Together these data exhibit how deep time proxies from paleosols can contribute to our knowledge and understanding of interactions among biotic, climatic, and atmospheric processes occurring at both regional and global scales while also providing crucial paleoclimatic, paleoatmospheric, and geochronological data for periods where greenhouse climate conditions persisted. Future work to constraint geochronology of the remaining fossil localities and increase stratigraphic coverage will continue to provide more resolution into the complex interaction of regional and global changes occurring during the Mid-Cretaceous transition in Texas and Oklahoma.

ACKNOWLEDGMENTS

We thank B. Barnett and M. Suarez for access to the Keck Palaeoenvironmental and Environmental Stable Isotope Lab at the University of Kansas and analyses of organic carbon samples. We thank L. Jacobs for his contributions and support for this research in addition to his exceptional mentoring over the years. This research was supported by NSF FRES 2121594 (CO2PIP Community Project) and funds from the Kansas Geological Survey.

AUTHOR CONTRIBUTIONS

KAA designed the project, compiled data, analyzed data, and drafted the manuscript, AM gathered data and analyzed data, and CRN collected samples. All authors edited the manuscript.

LITERATURE CITED

Ambrose, W. A., Hentz, T. F., Bonnaffe, F., Loucks, R. G., Brown, L. F. Jr., Wang, F. P., & Potter, E. C. (2009). Sequence-stratigraphic controls on complex reservoir architecture of highstand fluvial-dominated deltaic and lowstand valley-fill deposits in the Upper Cretaceous (Cenomanian) Woodbine Group, East Texas field: Regional and local perspectives. *AAPG Bulletin*, 93(2), 231–269. DOI 10.1306/09180808053.

Andrzejewski, K. A. & Tabor, N. J. (2020). Paleoenvironmental and paleoclimatic reconstruction of Cretaceous (Aptian-Cenomanian) terrestrial formations of Texas and Oklahoma using phyllosilicates. *Palaeogeography, Palaeoclimatology, Palaeoecology,* 543, 109491.

Andrzejewski, K. A., Tabor, N. J., Winkler, D., & Myers, T. S. (2022). Atmospheric pCO_2 reconstruction of Early Cretaceous terrestrial deposits in Texas and Oklahoma using pedogenic carbonate and occluded organic matter. *Geosciences*, 12, 148.

Arthur, M. A., Schlanger, S. O., & Jenkyns, H. C. (1987). The Cenomanian-Turonian oceanic anoxic event II, paleoceanographic controls on organic matter production and preservation. In J. Brooks & A. Fleet (Eds.), *Marine petroleum source rocks* (pp. 399–418), Geological Society Special Publication, 4. Oxford, UK: Blackwell.

Berquist, H. R. (1949). Geology of the Woodbine Formation of Cooke, Grayson and Fannin counties, Texas. In *Oil and Gas Investigations Map OM-98*. Reston: U.S. Geological Survey.

Breecker, D. O. (2017). Atmospheric pCO_2 control on speleothem stable carbon isotope compositions. *Earth and Planetary Science Letters*, 458, 58–68.

Cifelli, R. L., Gardner, J. D., Nydam, R. L., & Brinkman, D. L. (1997). Additions to the vertebrate fauna of the Antlers Formation (Lower Cretaceous), southeastern Oklahoma. *Oklahoma Geology Notes*, 57, 124–131.

Coccioni, R. & Galeotti, S. (2001). The mid-Cenomanian Event: the Prelude to the OAE2. *AGU Fall Meeting Abstracts* Vol. 2001.

Davies, S. M. (2015). Cryptotephras: The revolution in correlation and precision dating. *Journal of Quaternary Science*, 30(2), 114–130.

Dodge, C. F. (1952). Stratigraphy of the Woodbine Formation in the Arlington area. Tarrant County, TX. *Field and Laboratory*, 20, 66–78.

Dodge, C. F. (1968). Stratigraphic nomenclature of the Woodbine Formation Tarrant County, Texas. In C. F. Dodge (Eds.), *Field trip guidebook, south central section, stratigraphy of the Woodbine Formation, Tarrant County, Texas* (pp. 107–125). Geological Society of America.

Dodge, C. F. (1969). Stratigraphic nomenclature of the Woodbine Formation Tarrant County, Texas. *Texas Journal of Science*, 21, 43–62.

Emerson, B. L., Emerson, J. H., Akers, R. E., & Akers, T. J. (1994). *Texas Cretaceous Ammonites and Nautiloids*. Houston, Texas: Houston Gem and Mineral Society.

Gradstein, F. M., Ogg, J. G., & Smith, A. G. (2004). *A geologic time scale 2004*. UK: Cambridge University Press.

Gröcke, D. R., Ludvigson, G. A., Witzke, B. L., Robinson, S. A., Joeckel, R. M., Ufnar, D. F., & Ravn, R. L. (2006). Recognizing the Albian-Cenomanian (OAE1d) sequence boundary using plant carbon isotopes: Dakota Formation, Western Interior Basin, USA. *Geology*, 34(3), 193–196.

Hall, W. D. (1976). Hydrogeologic significance of depositional systems and facies in Lower Cretaceous sandstones, north-central Texas. *University of Texas, Austin, Bureau of Economic Geology Circular*, 76–1.

Haq, B. V., Hardenbol, J., & Vail, P. R. (1987). Chronology of fluctuating sea levels since the Triassic. *Science*, 235, 1159–1167.

Hare, V. J., Loftus, E., Jeffrey, A., & Ramsey, C. B. (2018). Atmospheric CO_2 effect on stable carbon isotope composition of terrestrial fossil archives. *Nature Communications*, 9(1), 1–8.

Hentz, T. F., Ambrose, W. A., & Smith, D. C. (2014). Eaglebine play of the southwestern East Texas basin: stratigraphic and depositional framework of the Upper Cretaceous (Cenomanian-Turonian) Woodbine and Eagle Ford Groups. *AAPG Bulletin*, 98(12), 2551–2580.

Hobday, D., Woodruff, C., & McBride., M. (1981). Paleotopographic and structural controls on non-marine sedimentation of the lower Cretaceous Antlers Formation and correlatives North Texas and Southeastern Oklahoma. *University of Texas, Austin, Bureau of Economic Geology Circular*, 71–87.

Hoke, G. D., Schmitz, M. D., & Bowring, S. A. (2014). An ultrasonic method for isolating non-clay components from clay-rich material. *Geochemistry, Geophysics, Geosystems*, 15, 492–498.

Jackson, S. E., Pearson, N. J., Griffin, W. L., & Belousova, E. A. (2004). The application of laser ablation-inductively coupled plasma-mass spectrometry to in situ U-Pb zircon geochronology. *Chemical geology*, 211(1-2), 47–69.

Jacobs, L. L. & Winkler, D. A. (1998). Mammals, archosaurs, and the Early to Late Cretaceous transition in north-central Texas. In Y. Tomida., L. J. Flynn, and L. L. Jacobs (Eds.), *Advances in vertebrate paleontology and geochronology* (pp. 253–280). National Science Museum, Tokyo.

Jenkyns, H. C. (1980). Cretaceous anoxic events: From continents to oceans. *Journal of Geological Society*, 137, 171-188. https://doi.org/10.1144/gsjgs.137/2/0171.

Jenkyns, H. C. (2010). Geochemistry of oceanic anoxic events. *Geochemistry Geophysics Geosystems*, 11, Q03004. https://doi.org/10.1029/2009GC002788

Joeckel, R. M., Suarez, C. A., Mclean, N. M., Möller, A., Ludvigson, G. A., Suarez, M. B., Kirkland, J. I., Andrew, J., Kiessling, S., & Hatzell, G. A. (2023). Berriasian-Valanginian geochronology and carbon-isotope stratigraphy of the Yellow Cat member, Cedar Mountain Formation, eastern Utah, USA. *Geosciences*, 13, 32. https://doi.org/10.3390/geoscienes13020032.

Johnson, R. O. (1974). *Lithofacies and depositional environments of the Rush Creek Member of the Woodbine Formation (Gulfian) of North Central Texas* [Unpublished M.S. thesis]. University of Texas.

Kauffman, E. G. & Caldwell, W. G. E. (1993). The Western Interior Basin in space and time. In: *Evolution of the Western Interior Basin: Geological Association of Canada*, [Special Paper]. 39, 1–30.

Kennedy, W. J. & Cobban, W. A. (1990). Cenomanian ammonite faunas from the Woodbine Formation and lower part of the Eagle Ford Group, Texas. *Palaeontology*, 33, 75–154.

Koch, P. L. (1998). Isotopic reconstruction of past continental environments. *Annual Review of Earth and Planetary Sciences*, 26(1), 573–613.

Kohn, M. J. (2010). Carbon isotope compositions of terrestrial C_3 plants as indicators of (paleo) ecology and (paleo) climate. *Proceedings of National Academy of Sciences*, 107(46), 19691–19695.

Lee, Y-N. (1997a). The archosauria from the Woodbine Formation (Cenomanian) in Texas. *Journal of Paleontology*, 71, 1147–1156. DOI 10.1017/S0022336000036088.

Lee, Y-N. (1997b). Bird and dinosaur footprints in the Woodbine Formation (Cenomanian). *Texas Cretaceous Research*, 18(6), 849–864. DOI 10.1006/cres.1997.0091.

Leandro, C. G., Savian, J. F., Kochhann, M. V. L., Franco, D. R., Coccioni, R., Frontalini, F., Gardin, S., Jovane, L., Figueiredo, M., Tedeschi, L. R., & Janikian, L. (2022). Astronomical tuning of the Aptian stage and its implications for age recalibrations and paleoclimate events. *Nature Communications*, 13(1), 2941.

Leckie, R. M, Bralower, T. J., & Cashman, R. (2002). Ocean anoxic events and plankton evolution: Biotic response to tectonic forcing during the mid-Cretaceous. *Paleoceanography*, 17(3), 13–1.

Ma, J. Y., Sun, W., Liu, X. N., & Chen, F. H. (2012). Variations in the stable carbon and nitrogen isotope composition of plants and soil along a precipitation gradient in northern China. *PloS One*, 7(12), e51894.

Main, D. J. (2009). Delta plain environments and ecology of the Cretaceous (Cenomanian) Woodbine Formation at the Arlington Archosaur Site, North Texas. *Geological Society of America, Abstracts with Programs*, 41, 103.

Murlin, J. R. (1975). *Stratigraphy and depositional environments of the Arlington Member, Woodbine Formation (Upper Cretaceous), Northeast Texas* [Unpublished M.S. Thesis]. University of Texas at Arlington, Arlington, TX, USA.

Myers, S. T., Tabor, N. J, Jacobs, L. L., & Bussert, R. (2016). Effects on different organic-matter sources on estimates of atmospheric and soil pCO_2 using pedogenic carbonate. *Journal of Sedimentary Research,* 86, 800–812.

Oliver, W. B. (1971). Depositional systems in the Woodbine Formation (Upper Cretaceous), northeast Texas: the University of Texas at Austin. *Bureau of Economic Geology Report of Investigations,* 73, 28. DOI 10.23867/RI0073D

Paces, J. B. & Miller Jr, J. D. (1993). Precise U-Pb ages of Duluth complex and related mafic intrusions, northeastern Minnesota: Geochronological insights to physical, petrogenetic, paleomagnetic, and tectonomagmatic processes associated with the 1.1 Ga midcontinent rift system. *Journal of Geophysical Research: Solid Earth*, 98(B8), 13997–14013.

Paton, C., Hellstrom, J., Paul, B., Woodhead, J., & Hergt, J. (2011). Iolite: Freeware for the visualization and processing of mass spectrometric data. *Journal of Analytical Atomic Spectrometry*, 26(12), 2508–2518.

Petrus, J. A. & Kamber, B. S. (2012). VizualAge: A novel approach to laser ablation ICP-MS U-Pb geochronology data reduction. *Geostandards and Geoanalytical Research*, 36(3), 247–270.

Powell, J. D. (1968). Woodbine-Eagle Ford transition, Tarrant Member. In C. F. Dodge (Eds.), *Stratigraphy of the Woodbine Formation: Tarrant County, Texas Field Trip Guidebook* (pp. 27–43). Geological Society of America, South Central Section.

Retallack, G. J. (1986). The fossil record of soils. In V. P. Wright (Eds.), *Paleosols: Their Recognition and Interpretation* (pp. 1–57). Blackwell Scientific Publications, Oxford.

Richey, J. D., Upchurch, G. R., Montañez, I. P, Lomax, B. H., Suarez, M. B., Crout, N. M. J., Joeckel, R. M., Ludvigson, G. A., & Smith, J. J. (2018). Changes in CO_2 during Ocean Anoxic Event 1d indicate similarities to other carbon cycle perturbations. *Earth and Planetary Science Letters*, 491, 172–182.

Schlanger, S. O. & Jenkyns, H. C. (1976). Cretaceous anoxic events: Causes and consequences. *Geologie et Mijnbouw*, 55, 179–184.

Schlanger, S. O., Arthur, M. A., Jenkyns, H. C., & Scholle, P. A. (1987).

The Cenomanian-Turonian Oceanic Anoxic Event, I. Stratigraphy and distribution of organic carbon-rich beds and the marine $\delta^{13}C$ excursion. In J. Brooks & A. J. Fleet (Eds.) *Marine petroleum source rocks*, *Geological Society Special Publication*, 26, 371-399. Oxford, UK: Blackwell. https://doi.org/10.1144/GSL.Sp.1987.026.01.24.

Schulz, E. D., Williams, R. J., Farquhar, G. D., Schulze, W., Langridge, J., Miller, J. M., & Walker, B. H. (1998). Carbon and nitrogen isotope discrimination and nitrogen nutrition of trees along a rainfall gradient in northern Australia. *Functional Plant Biology*, 25(4), 413–425.

Scott, C. (1940). Cephalopods from the Cretaceous Trinity Group of the south-central United States. *The University of Texas Bulletin*, 3945, 969−1125.

Sheldon, N. D. & Tabor, N. J. (2009). Quantitative paleoenvironmental and paleoclimatic reconstruction using paleosols. *Earth Science Reviews*, 95, 1−52.

Sláma, J., Košler, J., Condon, D. J., Crowley, J. L., Gerdes, A., Hanchar, J. M., & Whitehouse, M. J. (2008). Plešovice zircon: a new natural reference material for U-Pb and Hf isotopic microanalysis. *Chemical Geology*, 249(1-2), 1−35.

Slattery, J. S., Cobban, W. A., McKinney, K. C., Harries, P. J., & Sandness, A. L. (2015). Early Cretaceous to Paleocene paleogeography of the Western Interior Seaway: the interaction of eustasy and tectonism. In M. Bingle-Davis (Ed.), *Wyoming Geological Association Guidebook* (pp. 22−60). Casper, Wyoming.

Smith, J. J., Ludvigson, G. A., Layzell, A., Möller, A., Harlow, R. H., Turner, E., Platt, B., & Petronis, M. (2017). Discovery of Paleogene depostits of the central High Plains aquifer in the western Great Plains, USA. *Jounral of Sedimentary Resaerch*, 87(8), 880−896.

Swap, R. J., Aranibar, J. N., Dowty, P. R., Gilhooly, W. P., & Macko, S. A. (2004) Natural abundance of ^{13}C and ^{15}N in C_3 and C_4 vegetation of southern Africa: patterns and implications. *Global Change Biology*, 10, 350–358.

Tabor, N. J. & Myers, T. S. (2015). Paleosols as indicators of paleoenvironment and paleoclimate. *Annual Review Earth Planetary Sciences*, 43, 333–361.

Tabor, N. J., Myers, T. S., & Michel, L. A. (2017). Sedimentologist's guide for recognition, description, and classification of paleosols. In *Terrestrial depositional systems*. Elsevier. 165–208.

Trudel, P. (1994). *Stratigraphic sequences and facies architecture of the Woodbine-Eagle Ford interval, Upper Cretaceous, North Central Texas* [M.S. thesis] Tarleton State University, Stephenville, TX, USA.

Vermeesch, P. (2012). On the visualization of detrital age distributions. *Chemical Geology*, 312-313, 190–194.

Vermeesch, P. (2018). IsoplotR: A free and open toolbox for geochronology. *Geoscience Frontiers*, 9(5), 1479−1493.

Winkler, D. A., Murry, P. A., & Jacobs, L. L. (1990). Early Cretaceous (Comanchean) vertebrates of central Texas. *Journal of Vertebrate Paleontology*, 10, 95−116.

Winkler, D. A., Ruoff, K. A., Clemens, M. C., & Jacobs, L. L. (2015). Changes in small tetrapod faunas during the Early to Late Cretaceous transition in north-central Texas. *SVP Annual Meeting Program*. p. 239.

Wotzlaw, J. F., Schaltegger, U., Frick, D. A., Dungan, M. A., Gerdes, A., & Günther, D. (2013). Tracking the evolution of large-volume silicic magma reservoirs from assembly to supereruption. *Geology*, 41(8), 867−870.

Young, K. (1967). Comanche series (Cretaceous), south central Texas. Comanchean (Lower Cretaceous) Stratigraphy and Paleontology of Texas. *Permian Basin Section, Society of Economic Paleontologists and Mineralogists*, 67, 9−29.

Young, K. (1974). Lower Albian and Aptian (Cretaceous) ammonites of Texas. *Geoscience and Man*, 8, 175−228.

Young, K. (1986). Cretaceous, marine inundations of the San Marcos platform, Texas. *Cretaceous Research*, 7(2), 117−140.